

Tribology Characteristic of Ball Bearing SKF RB-12.7/G20W using SAE 5W-30 Lubricant with Carbon-Based Nanomaterial Addition

Poppy Puspitasari^{a,b,*}, Avita Ayu Permanasari^{a,b}, Muhammad Ilman Hakimi Chua Abdullah^c,
Diki Dwi Pramono^a, Oscar Jaya Silaban^a

^aDepartement of Mechanical and Industrial Engineering, Universitas Negeri Malang, Jl. Semarang No 5 Malang, Indonesia,

^bCentre of Advanced Materials for Renewable Energy, Universitas Negeri Malang, Jl. Semarang No 5 Malang, Indonesia,

^cFakulti Teknologi Kejuruteraan Mekanikal dan Pembuatan, Universiti Teknikal Malaysia Melaka, 76100 Durian Tunggal, Melaka, Malaysia.

Keywords:

Oil SAE 5W-30
Nanolubricant
Four-ball tribotester
Nanomaterial carbon
Wear morphology

* Corresponding author:

Poppy Puspitasari 
E-mail: poppy@um.ac.id

Received: 1 September 2023

Revised: 18 October 2023

Accepted: 27 November 2023

ABSTRACT

The thermophysical, rheological, and tribological properties in lubricant are essential for preserving the engines, power steering systems, and engine components from damage caused by friction and wear. The incorporation of nano-sized particles into lubricating oils has been reported to enhance these properties. Therefore, this study explores the impacts resulting from the incorporation of graphene, multiwalled carbon nanotubes (MWCNT), double-walled carbon nanotubes (DWCNT), and single-walled carbon nanotubes (SWCNT) at a quantity of 0.04 grams into the SAE 5W-30 base oil. These nanoparticles were synthesized using a two-step method, resulting in nanolubricants. The addition of carbon-based nanomaterials increases the density and decreases the viscosity of the base lubricant. The flow of nanolubricants exhibits non-Newtonian shear thinning behavior during the test at elevated temperatures. The results of the four-ball tribo-tester test reveal the increase of Coefficient of Friction (CoF) values and the extent of wear scar area. Further, the Scanning Electron Microscopy (SEM) analysis was employed to observe the wear morphology of the nanolubricants on the SKF RB-12.7/G20W ball bearing. Its results indicate a prevalence of groove-type wear as compared to conventional lubricants.

© 2023 Published by Faculty of Engineering

1. INTRODUCTION

Lubricants serve as the coating components which provide cooling and friction-mitigating effects for contact between component surfaces. Following technological advancements, lubricants that shield mechanical components from extreme

pressures exhibit enhanced resistance to friction-induced wear, and durability is necessary. Besides, the escalating production of motor vehicles from year to year poses a challenge in formulating lubricants capable of preserving the components. According to the Center Bureau of Statistics of Indonesia, the total number of motor vehicles has

increased significantly, from 133 million in 2019 to 136 million in 2020 and 141 million in 2021 [1]. In order to respond to this challenge, improvement in lubricant properties is crucial. Recent studies have reported that the combination of nanomaterials and lubricating oils can potentially elevate its features [2].

Nanolubricant constitutes a colloidal suspension that originates from the dispersion of nanoscale particles into base lubricant [3]. It is capable of mitigating friction and wear effectively. The incorporation of nanoparticles into lubricants as friction modifiers results in the nanospheres rolling behavior from the nanoparticle, formation of tribofilms through tribologically-induced chemical reactions, mending effects due to their minimum size, polishing effects [4], as well as synergistic and repairing effects [5]. Besides, the addition of nanoparticles has also been reported to enhance the stability of the lubricant [2,6] and reduce the viscosity as its viscosity index accelerates [7].

The addition of nanocarbon into lubricant oil has garnered profound interest from researchers as it offers excellent chemical stability, tribology properties and is environmentally friendly [5]. The mixture of graphene and multi-walled carbon nanotube (MWCNT) being dispersed into conventional oil lubricant enhances the tribology properties, reduces the friction coefficient, and distributes the load pressure among its constituent particles [8]. The study from Z. Said [9] uncovered that the addition of a single-walled carbon nanotube (SWCNT) with SDS surfactant into lubricant oil results in excellent stability with a higher thermal conductivity than the base fluid. Meanwhile, the SWCNT added with Carbon nanotube (CNT) also presents various forms and great stability to reduce friction and wear [10]. The study on the addition of CNT reveals that it affects the kinematic viscosity, pour point, tribological properties, and coefficient of thermal conductivity of gear oil [11].

In comparison to conventional lubricant oils, nanolubricant exhibit superior performance and operational characteristics. Following the attributes and characteristics offered by carbon nanomaterials as additives in lubricating oils, this study aims to ascertain the effects of incorporating graphene, MWCNT, DWCNT, and SWCNT into lubricant oils to enhance its performance. Further, the samples were characterized to identify their

density, dynamic viscosity, rheological attributes (including shear rate and shear stress, as well as tribological properties, such as the Coefficient of Friction (CoF), and wear. In the end, these obtained data were used to analyze the performance of base lubricating oil and the lubricant added with graphene, MWCNT, DWCNT, and SWCNT additives.

2. EXPERIMENTAL PROCEDURE

2.1 Material

In this study, the utilized nanomaterials were graphene, MWCNT, DWCNT, and SWCNT. Meanwhile, for the base lubricant oil, the SAE 5W-30 lubricant was adopted. This lubricant oil has been widely applied in various types of motor vehicles. The detailed information on each nanoparticle is presented in Table 1.

Table 1. Details of material used in this present study.

Name	Supplier	Purity [%]	Density [g/cm ³]	Diameter/ thickness [nm]
Engine oil 5W-30	Shell Advance	-	-	-
Graphene KNG-150	KNano	98	~0.15~0.2	<15
SWCNT	XFNano	>95	~0.14	5-10
DWCNT	XFNano	>95	~0.15	10-15
MWCNT	XFNano	>95	~0.19	25-30

Table 2. Property oil Shell ECO 5W-30 [12].

Property	Value
Kinematic Viscosity @40°C	59.1-62.1 cSt
Kinematic Viscosity @100°C	10.2-10.8 cSt
Density	845.3-848.3 kg/m ³
Flash Point	225 °C
Pour Point	-42 °C

2.2 Nanolubricants preparation

As studies on nanolubricant are continuously carried out, its excellent thermophysical properties have been confirmed. The available studies have reported that the excellent performance of nanofluid is affected by its optimum preparation method. In this study, we used a two-stage method for the nanolubricant preparation, as illustrated in Figure 1. The nanoparticle with 0.1% concentration was weighed and mixed with 200 ml of base oil using a magnetic stirrer at 1200 rpm for 15 minutes.

This two-stage method involved a set of techniques for improving the stability of the nanoparticle within the basic fluid, such as the sonication technique for 15 minutes using a KG-MT3N sonicator.

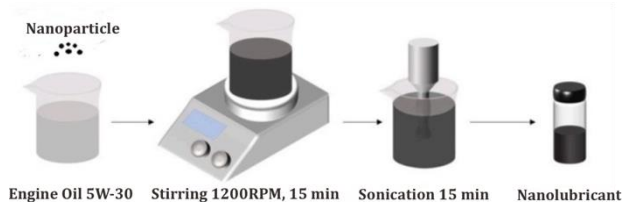


Fig. 1. Preparation of nanolubricant.

2.3 Nanoparticle characterization

The characteristics of Graphene, SWCNT, DWCNT, and MWCNT nanoparticles were analyzed using X-ray Diffraction (XRD) type E'xpert Pro, specifically to identify its crystal structure, crystallite size, and phase. Besides, the nanoparticles were also characterized using Scanning Electron Microscopy (SEM) type Inspect-S50 for the identification of the additive nanoparticles morphology. Another characterization using Fourier Transform Infra-Red (FTIR) type Irprestige 21 was also performed to identify functional groups and impurities.

2.4 Measurement of density and dynamic viscosity of nanolubricants

Density is typically represented by the symbol of ρ (rho). The density of the nanolubricant and the base lubricating oil were determined at equal volumes. The samples were subsequently weighed using the Optima Scale OPD-E 4-Decimal High Precision Analytical Balance. Further, the weighing results were calculated using Equation 1.

$$\rho = \frac{m}{V} \tag{1}$$

in which ρ represents the density of the fluid (kg/m^3), m is the mass (kg), and V is the volume (m^3).

In addition, dynamic viscosity, also known as absolute viscosity, was measured using the NDJ-8S viscometer. During the test, rotor no. 1 was employed, with varying rotor speeds of 6, 12, 30, and 60 rpm. For the test temperature, adhering to the ASTM 445 standards, kinematic viscosity tests were conducted at different temperatures of 40°C and 100°C due to the direct relationship between kinematic viscosity and dynamic viscosity.

2.5 Analysis of rheology of nanolubricants

The rheological properties were analyzed through the graph of the correlation between the shear stress and shear strain, as they carry a close relationship with the viscosity [13]. This graph aids the determination of the nature of fluid flow, whether it adheres to Newtonian or non-Newtonian behavior. In this rheological study, the lubricants were also subjected to test at both 40°C and 100°C temperatures. The shear rate was obtained using Equation 2.

$$\gamma = \frac{2\omega R_c^2 R_b^2}{x^2(R_c^2 - R_b^2)} \tag{2}$$

with γ representing the shear rate (/s), ω is the angular velocity of the spindle (rad/sec), R_c represents the vessel radius (cm), and R_b signifies the radius of the axis or spindle (cm). Meanwhile, the x refers to the exact radius at which the shear plane was being calculated. In this case, the x (cm) was equal to the R_b since the radius is measured starting from the same axis. The shear rate was estimated through Equation 3.

$$\tau = \gamma\mu \tag{3}$$

where τ is the shear stress (Pa), γ is the shear rate (/s) obtained from the calculation using Equation 2, and μ represents the dynamic viscosity (Pa.s). The dynamic viscosity was garnered using the NDJ-8S instrument. The rheology measurement is illustrated in Figure 2.

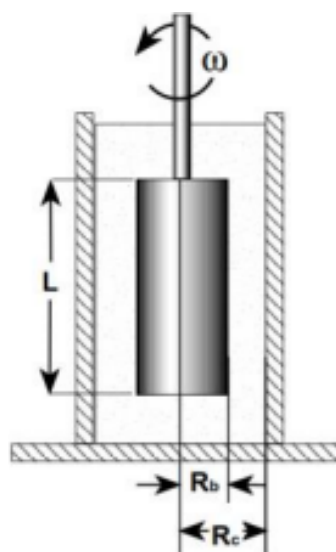


Fig. 2. Spindle and container for rheological measurements.

2.6 Tribology test

For identifying the Coefficient of Friction (CoF) and the wear friction, this study adopted four ball tribometer Koehler. The CoF test was performed using the ASTM D-5183 standard, with a rotational speed of 600 ± 60 rpm and load of $40,0 \pm 0,2$ kg, for 60 ± 1 minutes at $75 \pm 2^\circ\text{C}$. The ball bearing for the friction test was a ball bearing SKF RB-12.7/G20W. Further, SEM was conducted to observe the morphology of friction on the ball bearing. Further, the wear radius was examined using the microscope. The scheme of the four-ball test is illustrated in Figure 3.

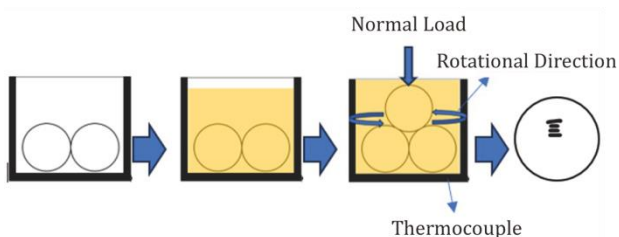


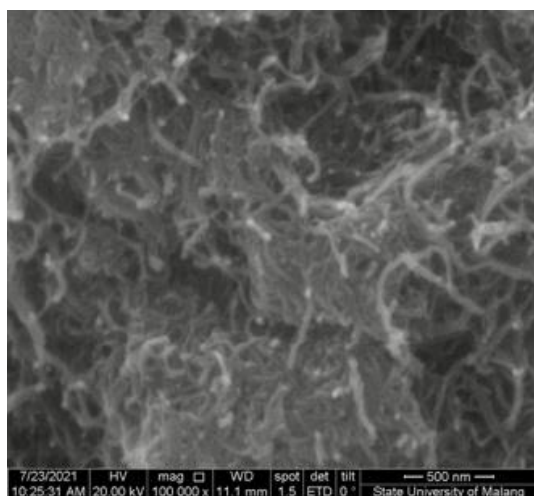
Fig. 3. Scheme of tribology test using four-ball tribometer.

3. RESULT AND DISCUSSION

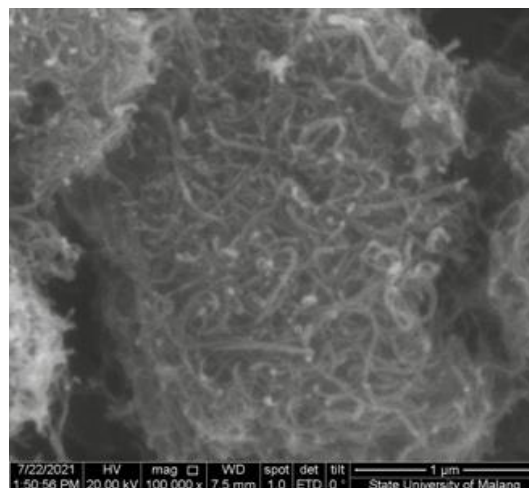
3.1 Nanoparticle characterization

3.1.1 Morphology of nanoparticles

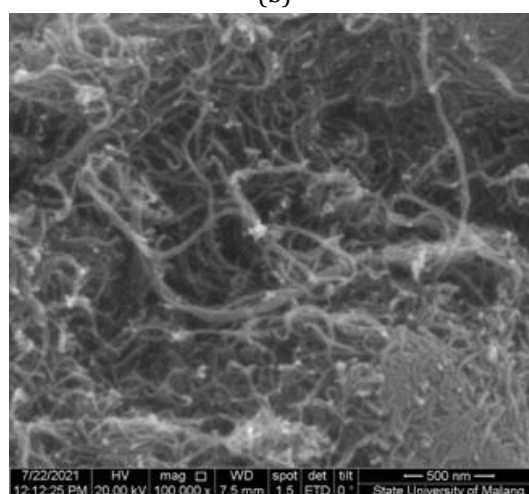
Scanning Electron Microscope (SEM) analysis was carried out on nanoparticle additives to investigate and identify their morphological structure [14]. SEM test results on magnifications of $100,000\times$ is shown in Fig. 4.



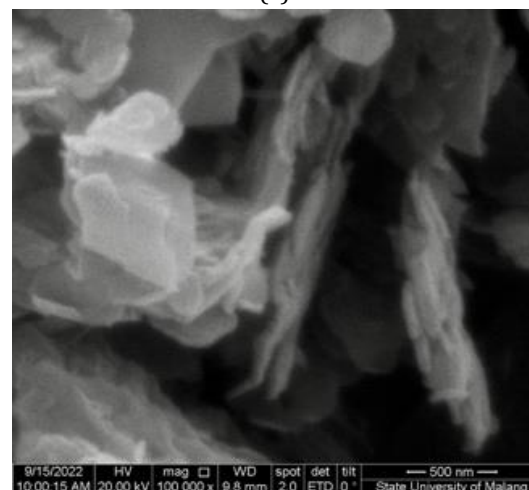
(a)



(b)



(c)



(d)

Fig. 4. SEM result of additive nanoparticle (a) MWCNT, (b) DWCNT, (c) SWCNT, and (d) Graphene.

The obtained morphology of nanoparticles is summarized in Figure 4. Based on Figure 4, MWCNT, DWCNT, and SWCNT have a wavy cylinder particle shape, with the presence of agglomerations, while Graphene nanoparticles have a platelet particle shape [15–17].

3.1.2 Phase of nanoparticles

XRD testing was performed at a diffraction angle of $10-90^\circ 2\theta$ and $\lambda = 1.54$ [18]. Figure 5 (a) and (b) are the XRD test results of the nanoparticle additives.

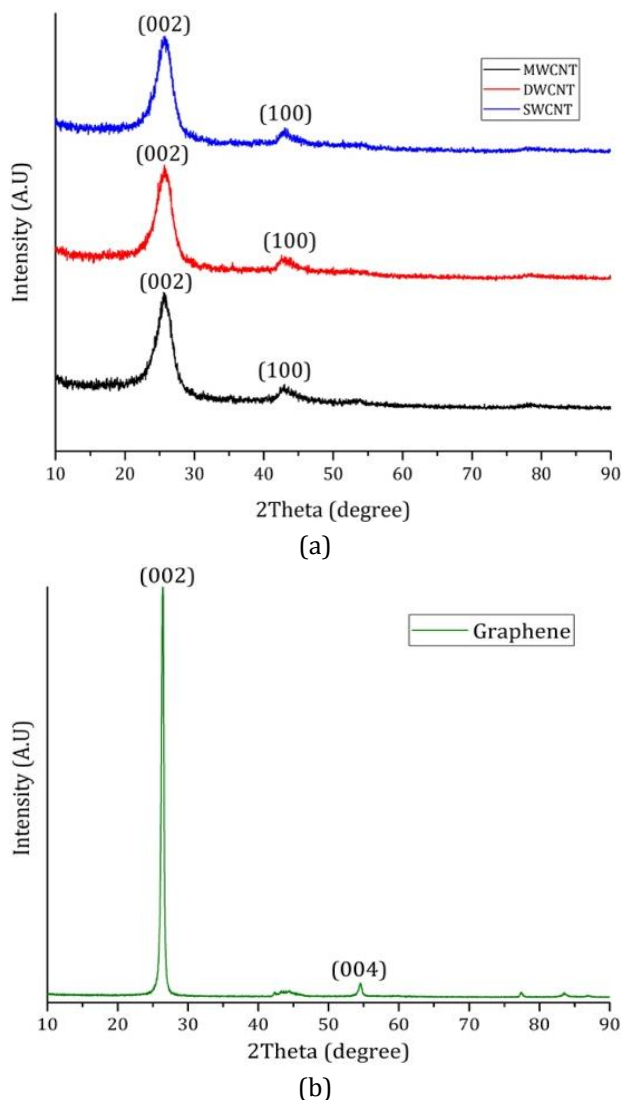


Fig. 5. XRD result of additive nanoparticle (a) MWCNT, DWCNT, SWCNT, and (b) Graphene.

Figure 5 (a) shows the MWCNT, DWCNT, and SWCNT nanoparticle additive samples, where a peak appears at $2\theta = 26^\circ$, indicating the presence of carbon at the reflection plane (002) [19–21]. Besides, MWCNT, DWCNT, and SWCNT samples also show a peak at $2\theta = 42.4^\circ$, which is the reflection plane (100) [22].

Based on Figure 5 (b), the Graphene nanoparticle additive sample exhibits a peak at $2\theta = 26.2$ and 54.5° which is the reflection plane (002) and (004), respectively, from carbon and strongly confirms graphene [23,24].

3.1.3 Functional groups of nanoparticles

FTIR testing was carried out at a wavelength of $4000 - 400 \text{ cm}^{-1}$ [25]. Figure 6 illustrates the result of the FTIR test on the nanoparticle additive samples.

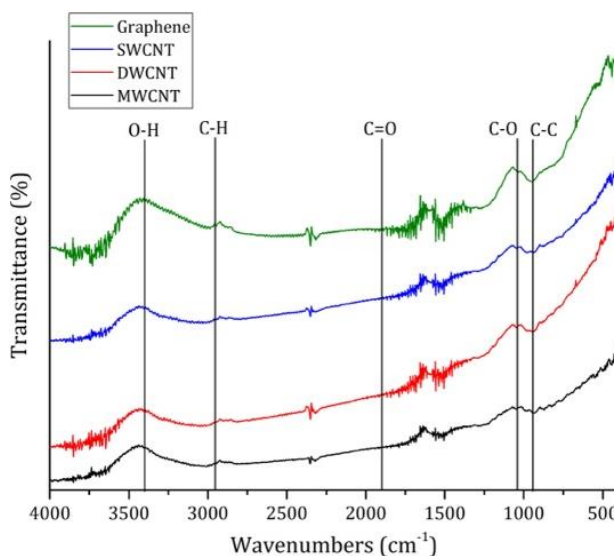


Fig. 6. FTIR result of additive nanoparticle MWCNT, DWCNT, SWCNT, and Graphene.

Based on Figure 6, in the MWCNT, DWCNT, SWCNT, and graphene nanoparticle additive samples, there is an absorption peak at wavenumber $3358.07-3584.73 \text{ cm}^{-1}$, indicating the O–H stretching of the terminal carboxyl group [26]. Another absorption peak was observed at wavelength $2954.95-2985.81 \text{ cm}^{-1}$ indicating the C–H stretching [27]. Another peak was also detected at wavenumber $1865.17-1886.38 \text{ cm}^{-1}$, implying the carboxyl C=O bond stretching [28]. The pointed transmittances at 1145.72 cm^{-1} and 1099.43 cm^{-1} were ascribed to the C–O stretching of the secondary hydroxyl and primary oxhydryl [29]. Other peaks were also present at wavenumbers $927.76-941.26 \text{ cm}^{-1}$, signifying the C–C stretching [30].

3.2 Density of nanolubricants

The obtained density for the nanolubricant samples is illustrated in Figure 7. These data were estimated through Equation 1. The data suggest that the addition of nanoparticles improves the density of basic lubricating oil. The highest density was obtained from the nanolubricant with the addition of SWCNT, reaching 826.67 kg/m^3 , while the density of the nanolubricant with MWCNT was 816.67 kg/m^3 ,

followed by nanolubricant with DWCNT sample by 806.67 kg/m³ and nanolubricant with graphene by 803.33 kg/m³. Further, we identified that the SAE 5W-30 lubricant presents a density of 752.21 kg/m³. Therefore, the addition of nanomaterial into the lubricant oil enhances the density of the basic lubricating oil.

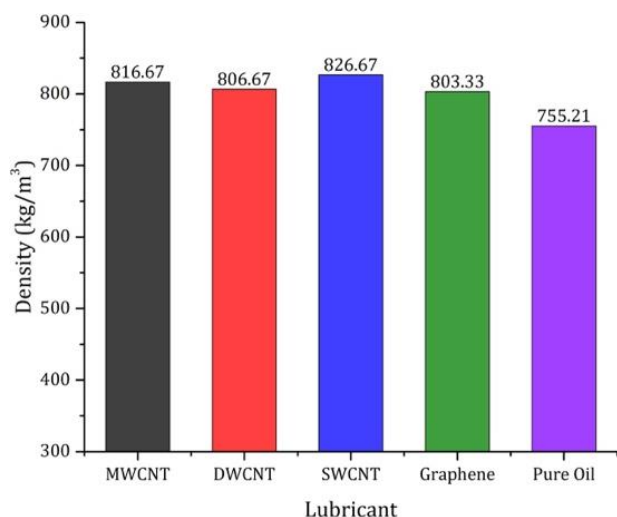


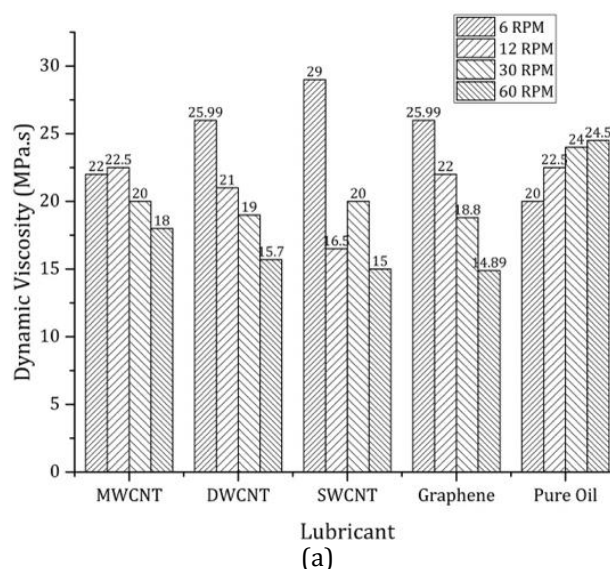
Fig. 7. Density of sample lubricant.

3.3 Dynamic viscosity of nanolubricants

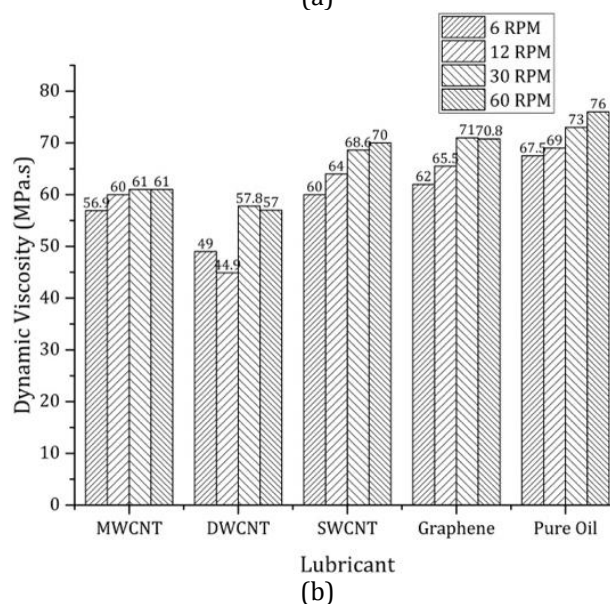
The viscosity of a fluid is significantly influenced by temperature. Besides, at higher temperatures, viscosity tends to be lower and vice versa, as shown in Figure 8. The dynamic viscosity of nanolubricant at 100°C and a rotational speed of 30 rpm are 20, 19, 20, and 18.8 for each respective nanolubricant variant with MWCNT, DWCNT, SWCNT, and graphene addition, respectively. The addition of carbon nanomaterials also tends to decrease the viscosity values, as presented in Figure 4a. At 100°C and a rotational speed of 30 rpm, the base lubricating oil has a dynamic viscosity of 24 MPa.s. Meanwhile, at the same rotational speed and 40°C temperature, its viscosity remains consistent at 73 MPa.s.

In addition, the rotational speed of the spindle also affects viscosity. Figure 8 presents that as the spindle rotates faster at 100°C, the viscosity decreases. This aligns with the finding reported by Nintyas & Caesaron, 2015 [31] that with the increase of the spindle's rotation speed, the viscosity read by the viscometer decreases. Conversely, the slower spindle rotation pace results in higher viscosity measured by the viscometer. However, at lower temperatures, such

as 40°C, we observed a conversed finding, in which faster spindle rotation leads to higher viscosity. Meanwhile, Devrani et al., 2017 [32] uncovered that more significant effort from the spindle is required to achieve the same rotational speed at the tip, resulting in a lower level of strain.



(a)



(b)

Fig. 8. Dynamic Viscosity of Nanolubricant and Base Lubricating Oil at Different Temperatures of: (a) 100°C and (b) 40°C.

3.4 Rheology of nanolubricants

Figure 9 shows the comparison of shear stress values against the shear rate for each specimen. Linear graphs indicate Newtonian behavior, while non-linear graphs suggest non-Newtonian behavior [33]. At 100 and 40°C, the base lubricating oil exhibits Newtonian flow characteristics. In contrast to the base lubricating

oil, nanolubricants yield different behavior under the two temperature conditions. At 40°C, all nanolubricant specimens present Newtonian flow, as presented in Figure 9b. However, at 100°C, there is a transition from Newtonian to non-Newtonian fluid behavior. In specific, the non-Newtonian flow properties exhibited across all nanolubricant specimens reveal a non-Newtonian shear thinning behavior. Further, Chinyoka, 2021 [34] described that at a higher temperature, the shear thinning of nanolubricant also increases. Shear thinning is a non-Newtonian fluid property representing the higher shear rate of the fluid. The alteration in flow behavior observed in this nanolubricant resembles the SAE 5W-40 lubricant, which also presents the non-Newtonian shear thinning property at elevated temperatures [35]. Generally, lubrication oil with Newtonian properties presents an excellent performance in preventing friction and wear while also enhancing the load capacity of a component. Meanwhile, the non-Newtonian fluid applied on the bearing reduces its noise [36] and improves load-carrying capacity, as well as lowering contact friction [37]. Davies and Walters [38], describing non-Newtonian fluid mechanics, uncovered that normal stresses acting in the flow direction contribute additional load-carrying stresses in this geometry. In non-Newtonian fluids, the flowing internal friction distorts the temporary network structure formed by entangled molecules and, in general, aligns molecular segment elements between cross-links in the flow direction. As a result of the network structure being stretched, this deformation generates a set of forces (or stresses if the forces are normalized by their area of action) within the fluid that acts along the line of flow and perpendicular to the flow (called normal stresses) [38,39].

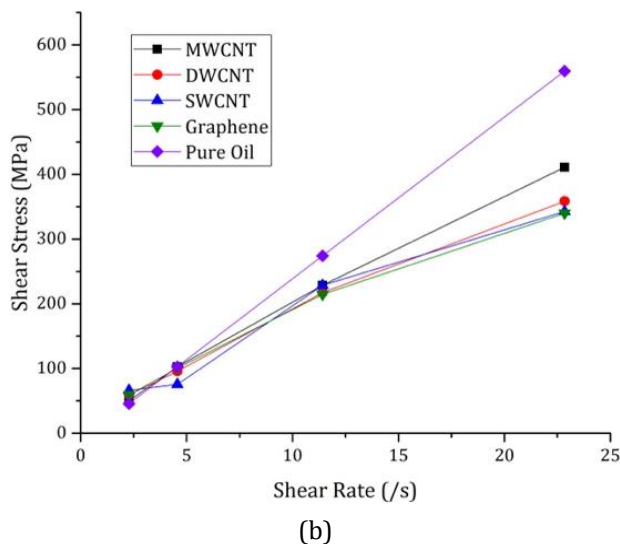
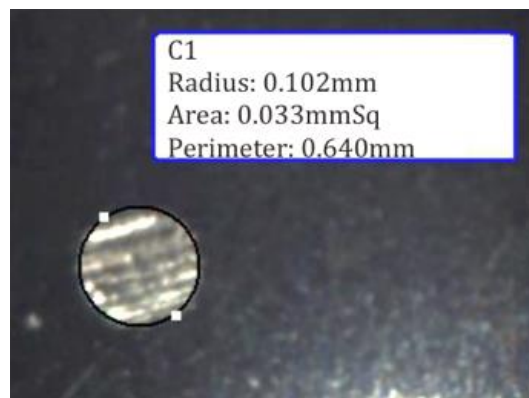
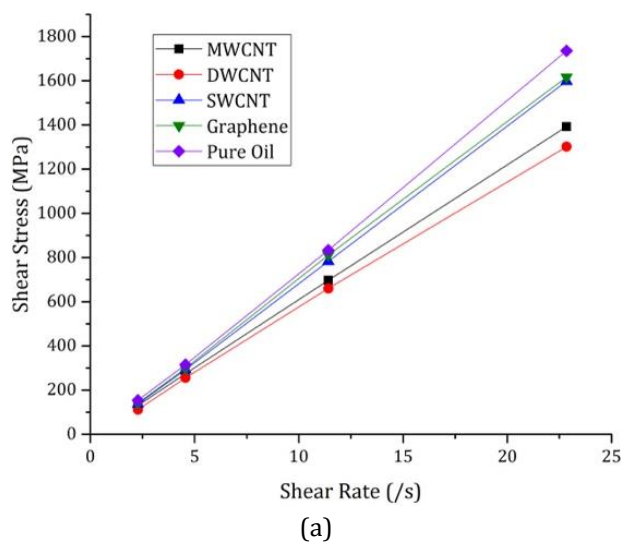


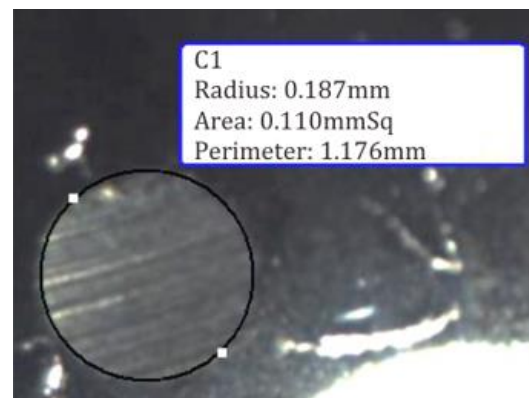
Fig. 9. Comparison of shear rate and shear stress on each nanolubricant sample and basic lubricating oil at temperatures of (a) 100°C and (b) 40°C.

3.5 Tribology properties

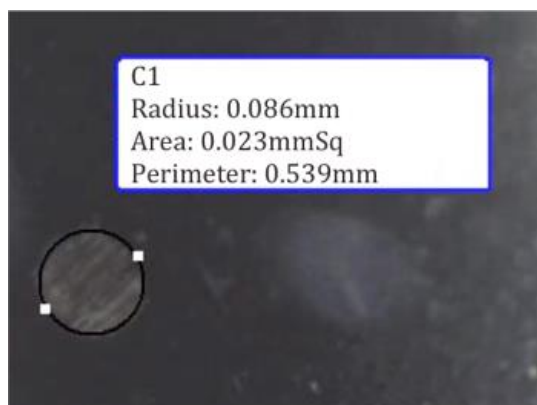
Figure 10. shows the results of friction observed using a microscope, which includes the radius, area, and wear perimeter caused by friction that occurs when carrying out tests using a four-ball machine with nanolubricant media, while the radius and the wear area were analyzed using the microscope.



(a)



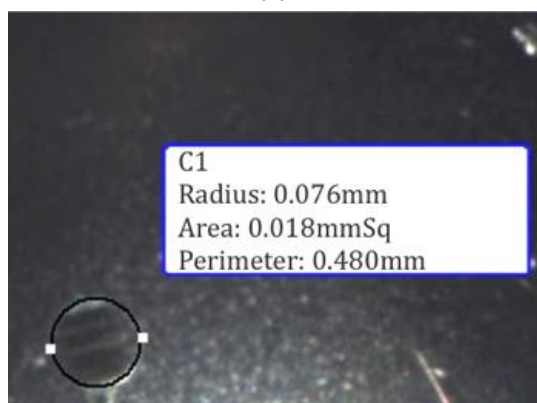
(b)



(c)



(d)



(e)

Fig. 10. Friction area of Ball Bearing after four-ball tests with nanolubricant (a) MWCNT, (b) DWCNT, (c) SWCNT, (d) Graphene and (e) Pure Oil SAE 5W-30.

Table 3. Wear radius and wear area result of ball bearing after four ball tests with samples lubricant.

Sample Lubricant	Average Wear Radius (mm)	Average Wear Area (mm ²)
MWCNT	0.099	0.031
DWCNT	0.140	0.065
SWCNT	0.086	0.024
Graphene	0.100	0.032
Pure Oil	0.084	0.022

Figure 10 and Table 3 show the value of the radius and the area of wear that occurs due to friction on the ball bearings being used. The value of pure SAE 5W-30 lubricant produces an average wear radius of 0.084 mm and an average wear area of 0.022 mm². In the nanolubricant, the largest average radius and average area were produced by the DWCNT nanolubricant with an average value of 0.140 mm and an average area of 0.065 mm², while the smallest was the SWCNT nanolubricant with an average radius value 0.086 mm radius and an average area of 0.024 mm². The increase in the diameter of the wear marks can be caused by non-uniformity and agglomeration of the nanomaterial when mixed with base oil [6].

The four-ball tribometer was used to measure the CoF on the pressure. Based on Table 3 and Figure 11, the growth of the radius tends to be followed by the increase of CoF. The test results indicate varying CoF and wear radius. Based on Figure 11, it can be observed that the pure lubricant sample has the lowest CoF value when compared to the lubricant sample with additional nanoparticle additives. The lubricant sample with MWCNT has a CoF value of 0.078, while the lubricant sample with DWCNT has a CoF value of 0.093, and the lowest CoF value among lubricants with nanoparticle additives is owned by the lubricant sample with SWCNT of 0.075. The highest CoF value is observed on the lubricant sample with graphene of 0.099.

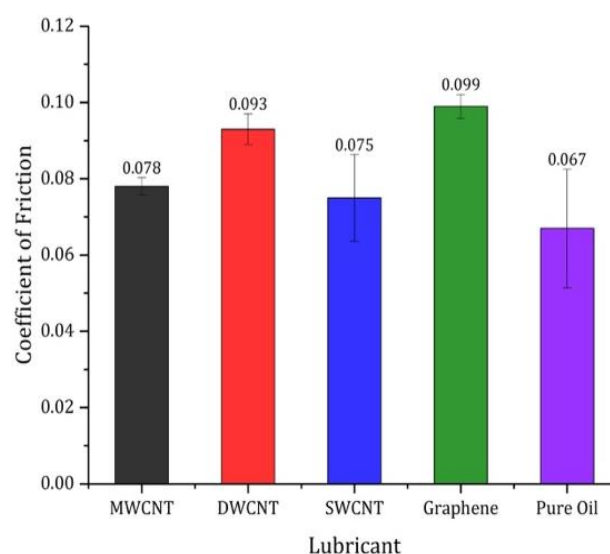


Fig. 11. Coefficient of friction (CoF) of samples nanolubricant.

A large CoF value does not indicate that the resulting wear will be as significant as graphene nanolubricant, which shows the largest CoF value but produces lower wear marks than DWCNT, which has lower CoF. As explained by [41], the existing CoF value does not depend on the visible contact area. This also supports the statement from Blau, 2001 [42], which describes that the time to achieve frictional break-in and wear are generally not the same. That is, there is an interesting interaction between friction, wear, and tear as the tribosystem ages. Blau, 2001 [42] gave an example that frictional friction can cause the accumulation of damage to the point of breaking, at which time the particles are released. The particles change the frictional resistance, which in turn affects the energy available to generate and expel the particles continuously. Meanwhile, the interfacial temperature can increase and change the mechanical properties and surface reactivity.

An increase in the coefficient of friction has been reported in a study by Kamel, et al. 2021 [6] when SAE 5W-30 lubricant was mixed with MWCNT nanofluid. This finding demonstrates that adding nanofluids to lubricants can increase friction, as measured by the CoF value. The study further described that the wear marks and surface deformation of the MWCNT nanolubricant were higher than the base oil lubricant, namely SAE 5W-30. The wear marks under base oil lubrication consist of visible furrows and channels, whereas the wear marks on the nanolubricant are smooth with shallow grooves. Likewise, Syahrullail et al., 2013 [43] found that adding palm fatty acid distillate into commercial metal-forming increased the diameter of wear marks in the area of the wear marks diameter test when compared to pure CMFO. The study also concluded no correlation or relationship between CoF and the diameter of the wear mark, which was caused by oxidation.

The direct correlation between the Coefficient of Friction (CoF) and wear radius cannot be conclusively established as they have no direct connection [41]. In specific applications, such as constructing stable table legs, a high CoF is essential to prevent the shift of the table. However, for lubricants, the tendency of high CoF indicates inadequate surface protection from wear due to friction [44].

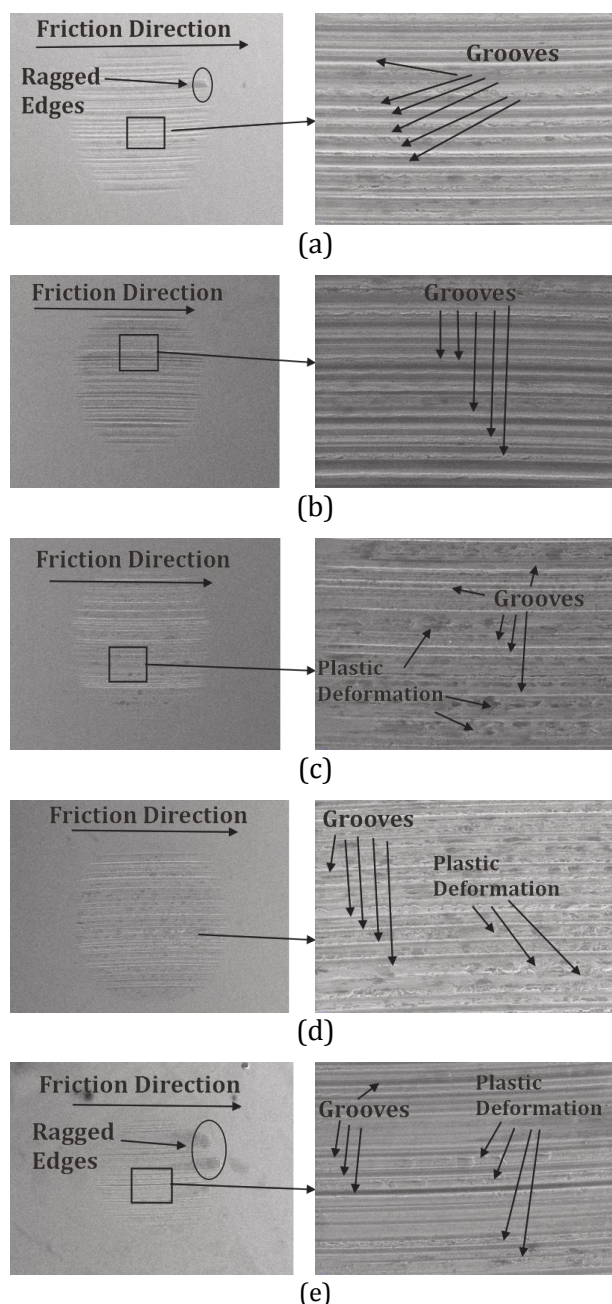


Fig. 12. SEM results obtained from ball bearing SKF RB-12.7/G20W test for nanolubricant with (a) MWCNT; (b) DWCNT; (c) SWCNT; (d) Graphene; and (e) Pure oil SAE 5W-30.

Abrasive wear was identified by the presence of grooves, while adhesive wear was characterized by plastic deformation. The friction results are dominated by abrasive wear, as confirmed by the presence of numerous grooves. The nanolubricant with MWCNT addition and the base lubricating oil SAE 5W-30 exhibit the most excellent worn surfaces among the samples. This could be attributed to three-body abrasion and is likely a consequence of oxide products and wear debris (particles) that engage in frictional

interactions [44]. The nanolubricant with MWCNT addition experiences abrasive wear indicated by slight signs of wear on the edges, as shown in Figure 12. Meanwhile, Figure 12b illustrates that the nanolubricant with DWCNT tends to produce more pronounced and deeper abrasive wear, as observed from the darker lines than the lines from other samples. Further, the nanolubricant with SWCNT addition exhibits well-defined edges with wear which is predominantly influenced by abrasive wear, as shown in Figure 12c. Besides, this sample also has several adhesive wear, albeit not as prominent as the adhesive wear observed in the nanolubricant with graphene. Figure 12d shows that the nanolubricant with graphene additive has a unique outcome since it displays the highest incidence of adhesive wear, although still primarily dominated by abrasive wear.

4. CONCLUSION

Our analysis results suggested that the addition of carbon nanomaterial transforms the properties of basic lubricating oil, specifically in its density, viscosity, rheology, and tribological properties.

The nanolubricant possesses a higher density than the base lubricating oil. Meanwhile, the particle density significantly influences the lubricant's viscosity at different temperatures. Consequently, the lubricant with higher viscosity at elevated temperatures is more desirable, as it offers better protection against friction and wear in the machine. At high temperatures, nanolubricant with MWCNT additive demonstrates improved viscosity compared to nanolubricants with other additives, yet it falls short of the performance of SAE 5W-30 oil. Besides, at high temperatures, the flow of nanolubricant shifts from Newtonian into Non-Newtonian shear thinning as caused by the increase of shear rate at the increasing temperature. Further, nanolubricants exhibit higher wear traces and increased Coefficient of Friction (CoF) compared to base lubricating oil. This is attributed to the lack of homogeneity in the lubricant and the presence of agglomerated particles. The observed wear indicates abrasive wear, possibly caused by wear debris gripping and leaving marks during friction.

Acknowledgment

We would like to address our gratitude to Universitas Negeri Malang for the Matching Fund Grant (5.4.864/UN32.20.1/LT/2023).

REFERENCES

- [1] Badan Pusat Statistik, "Perkembangan Jumlah Kendaraan Bermotor Menurut Jenis (Unit), 2019-2021." Accessed: May 03, 2023. [Online]. Available: <https://www.bps.go.id/indicator/17/57/1/perkembangan-jumlah-kendaraan-bermotor-menurut-jenis.html>
- [2] A. S. Al-Janabi, M. H. Hussin, and M. Z. Abdullah, "Stability, thermal conductivity and rheological properties of graphene and MWCNT in nanolubricant using additive surfactants," *Case Studies in Thermal Engineering*, vol. 28, p. 101607, Dec. 2021, doi: 10.1016/j.csite.2021.101607.
- [3] W. K. Shafi and Charoo, "NanoLubrication Systems: An Overview," *Materials Today: Proceedings*, vol. 5, no. 9, pp. 20621–20630, Jan. 2018, doi: 10.1016/j.matpr.2018.06.443.
- [4] W. Dai, B. Kheireddin, H. Gao, and H. Liang, "Roles of nanoparticles in oil lubrication," *Tribology International*, vol. 102, pp. 88–98, Oct. 2016, doi: 10.1016/j.triboint.2016.05.020.
- [5] J. Zhao, Y. Huang, Y. He, and Y. Shi, "Nanolubricant additives: A review," *Friction*, vol. 9, no. 5, pp. 891–917, Dec. 2020, doi: 10.1007/s40544-020-0450-8.
- [6] B. M. Kamel et al., "Optimization of the Rheological Properties and Tribological Performance of SAE 5w-30 Base Oil with Added MWCNTs," *Lubricants*, vol. 9, no. 9, p. 94, Sep. 2021, doi: 10.3390/lubricants9090094.
- [7] E. R. Zvereva, R. V. Khabibullina, G. R. Akhmetvalieva, A. O. Makarova, and O. S. Zueva, "Influence of Nanoadditives on Rheological Properties of Fuel Oil," *Advances in Engineering Research*, vol. 133, pp. 914–920, Jan. 2017, doi: 10.2991/aime-17.2017.148.
- [8] L. Joly-Pottuz, F. Dassenoy, B. Vacher, J. M. Martin, and T. Mieno, "Ultralow friction and wear behaviour of Ni/Y-based single wall carbon nanotubes (SWNTs)," *Tribology International*, vol. 37, no. 11–12, pp. 1013–1018, Nov. 2004, doi: 10.1016/j.triboint.2004.07.019.
- [9] Z. Said, "Thermophysical and optical properties of SWCNTs nanofluids," *International Communications in Heat and Mass Transfer*, vol. 78, pp. 207–213, Nov. 2016, doi: 10.1016/j.icheatmasstransfer.2016.09.017.

- [10] A. Mohamed, S. F. Ali, T. A. Osman, and B. M. Kamel, "Development and manufacturing an automated lubrication machine test for nano grease," *Journal of Materials Research and Technology*, vol. 9, no. 2, pp. 2054–2062, Mar. 2020, doi: [10.1016/j.jmrt.2019.12.038](https://doi.org/10.1016/j.jmrt.2019.12.038).
- [11] W. Khalil, A. Mohamed, M. A. Bayoumi, and T. A. Osman, "Thermal and rheological properties of industrial mineral gear oil and Paraffinic Oil/CNTs nanolubricants," *Iranian Journal of Science and Technology, Transactions of Mechanical Engineering*, vol. 42, no. 4, pp. 355–361, Jun. 2017, doi: [10.1007/s40997-017-0103-3](https://doi.org/10.1007/s40997-017-0103-3).
- [12] Shell, "Shell ECO 5W-30." Shell Lubricants. Accessed: Sep. 09, 2023. [Online]. Available: https://solutions.shell.com/id/products/Helix_ECO_5W-30_001G6995
- [13] A. K. Sharma, A. K. Tiwari, and A. R. Dixit, "Rheological behaviour of nanofluids: A review," *Renewable & Sustainable Energy Reviews*, vol. 53, pp. 779–791, Jan. 2016, doi: [10.1016/j.rser.2015.09.033](https://doi.org/10.1016/j.rser.2015.09.033).
- [14] P. Puspitasari and D. D. Pramono, "Phase identification, morphology, and compressibility of scallop shell powder (Amusium pleuronectes) for bone implant materials," in *CRC Press eBooks*, 2022, pp. 5–25. doi: [10.1201/9781003320746-2](https://doi.org/10.1201/9781003320746-2).
- [15] M. C. G. Pedrosa, J. C. D. Filho, L. R. De Menezes, and E. O. Da Silva, "Chemical surface modification and characterization of carbon nanostructures without shape damage," *Materials Research-ibero-american Journal of Materials*, vol. 23, no. 2, Jan. 2020, doi: [10.1590/1980-5373-mr-2019-0493](https://doi.org/10.1590/1980-5373-mr-2019-0493).
- [16] M. Zhang and J. Li, "Carbon nanotube in different shapes," *Materials Today*, vol. 12, no. 6, pp. 12–18, Jun. 2009, doi: [10.1016/s1369-7021\(09\)70176-2](https://doi.org/10.1016/s1369-7021(09)70176-2).
- [17] M. G. Ivanov et al., "Nanodiamond-Based nanolubricants," *Fullerenes, Nanotubes, and Carbon Nanostructures*, vol. 20, no. 4–7, pp. 606–610, May 2012, doi: [10.1080/1536383x.2012.657010](https://doi.org/10.1080/1536383x.2012.657010).
- [18] D. D. Pramono, P. Puspitasari, A. A. Permasari, S. Sukarni, and A. Wahyudiono, "Effect of sintering time on porosity and compressibility of calcium carbonate from Amusium pleuronectes (scallop shell)," *Nucleation and Atmospheric Aerosols*, Jan. 2023, doi: [10.1063/5.0120990](https://doi.org/10.1063/5.0120990).
- [19] M.-S. Park, K. H. Kim, and Y.-S. Lee, "Fluorination of single-walled carbon nanotube: The effects of fluorine on structural and electrical properties," *Journal of Industrial and Engineering Chemistry*, vol. 37, pp. 22–26, May 2016, doi: [10.1016/j.jiec.2016.03.024](https://doi.org/10.1016/j.jiec.2016.03.024).
- [20] Y. T. Prabhu, K. V. Rao, B. S. Kumari, V. S. Sai, and T. Pavani, "Nickel and nickel oxide nanocrystals selectively grafting on multiwalled carbon nanotubes," *Nano Convergence*, vol. 2, no. 1, Jan. 2015, doi: [10.1186/s40580-014-0038-y](https://doi.org/10.1186/s40580-014-0038-y).
- [21] V. Thirumal, A. Pandurangan, R. Jayavel, S. Krishnamoorthi, and R. Ilangovan, "Synthesis of nitrogen doped coiled double walled carbon nanotubes by chemical vapor deposition method for supercapacitor applications," *Current Applied Physics*, vol. 16, no. 8, pp. 816–825, Aug. 2016, doi: [10.1016/j.cap.2016.04.018](https://doi.org/10.1016/j.cap.2016.04.018).
- [22] P. M. Masipa, T. Magadzu, and B. Mkhondo, "Decoration of Multi-walled Carbon Nanotubes by Metal Nanoparticles and Metal Oxides using Chemical Evaporation Method," *South African Journal of Chemistry*, vol. 66, pp. 173–178, May 2013.
- [23] B. Wang and S. Deng, "Effect and mechanism of graphene nanoplatelets on hydration reaction, mechanical properties and microstructure of cement composites," *Construction and Building Materials*, vol. 228, p. 116720, Dec. 2019, doi: [10.1016/j.conbuildmat.2019.116720](https://doi.org/10.1016/j.conbuildmat.2019.116720).
- [24] M. Rashad, F. Pan, M. Asif, and X. Chen, "Corrosion behavior of magnesium-graphene composites in sodium chloride solutions," *Journal of Magnesium and Alloys*, vol. 5, no. 3, pp. 271–276, Sep. 2017, doi: [10.1016/j.jma.2017.06.003](https://doi.org/10.1016/j.jma.2017.06.003).
- [25] J. Maulana, H. Suryanto, and A. Aminuddin, "Effect of graphene addition on bacterial Cellulose-Based nanocomposite," *Journal of Mechanical Engineering Science and Technology (JMEST)*, vol. 6, no. 2, p. 107, Nov. 2022, doi: [10.17977/um016v6i2022p107](https://doi.org/10.17977/um016v6i2022p107).
- [26] C. E. Pizzutto, J. Suave, J. Bertholdi, S. H. Pezzin, L. B. N. Coelho, and S. C. Amico, "Study of epoxy/CNT nanocomposites prepared via dispersion in the hardener," *Materials Research-ibero-american Journal of Materials*, vol. 14, no. 2, pp. 256–263, Jun. 2011, doi: [10.1590/s1516-14392011005000041](https://doi.org/10.1590/s1516-14392011005000041).
- [27] X. Zhao, R. Liu, Z. Chi, Y. Teng, and P. Qin, "New Insights into the Behavior of Bovine Serum Albumin Adsorbed onto Carbon Nanotubes: Comprehensive Spectroscopic Studies," *Journal of Physical Chemistry B*, vol. 114, no. 16, pp. 5625–5631, Apr. 2010, doi: [10.1021/jp100903x](https://doi.org/10.1021/jp100903x).
- [28] M. J. Yee, N. M. Mubarak, M. Khalid, E. C. Abdullah, and P. Jagadish, "Synthesis of polyvinyl alcohol (PVA) infiltrated MWCNTs buckypaper for strain sensing application," *Scientific Reports*, vol. 8, no. 1, Nov. 2018, doi: [10.1038/s41598-018-35638-3](https://doi.org/10.1038/s41598-018-35638-3).

- [29] S. Zhang et al., "Multiwall-carbon-nanotube/cellulose composite fibers with enhanced mechanical and electrical properties by cellulose grafting," *RSC Advances*, vol. 8, no. 11, pp. 5678–5684, Jan. 2018, doi: [10.1039/c7ra11304h](https://doi.org/10.1039/c7ra11304h).
- [30] B. Xue et al., "Functionalized multiwalled carbon nanotubes by loading phosphorylated chitosan," *High Performance Polymers*, vol. 30, no. 9, pp. 1036–1047, Nov. 2017, doi: [10.1177/0954008317736375](https://doi.org/10.1177/0954008317736375).
- [31] S. S. A. Nintyas and D. Caesaron, "Pengaruh Kecepatan Putar Spindel Dalam Dengan Metode Anova," *Journal of Industrial Engineering & Management System*, vol. 8, no. 1, pp. 70–78, 2015.
- [32] S. Devrani, R. Sharma, M. Rajesh, and A. Kapoor, "Exploring viscoelastic characteristics of Polymer-Water solutions by viscometric analysis," *Asian Journal of Chemistry*, vol. 29, no. 9, pp. 1953–1958, Jan. 2017, doi: [10.14233/ajchem.2017.20646](https://doi.org/10.14233/ajchem.2017.20646).
- [33] M. Sepehrnia, M. J. Farrokh, M. Karimi, and K. Mohammadzadeh, "Experimental study and development of mathematical model using surface response method to predict the rheological performance of CeO₂-CuO/10W40 hybrid nanolubricant," *Arabian Journal of Chemistry*, vol. 16, no. 6, p. 104721, Jun. 2023, doi: [10.1016/j.arabjc.2023.104721](https://doi.org/10.1016/j.arabjc.2023.104721).
- [34] T. Chinyoka, "Comparative response of Newtonian and Non-Newtonian fluids subjected to exothermic reactions in shear flow," *International Journal of Applied and Computational Mathematics*, vol. 7, no. 3, Apr. 2021, doi: [10.1007/s40819-021-01023-4](https://doi.org/10.1007/s40819-021-01023-4).
- [35] A. A. Nadooshan, M. H. Esfe, and M. Afrand, "Evaluation of rheological behavior of 10W40 lubricant containing hybrid nano-material by measuring dynamic viscosity," *Physica E: Low-dimensional Systems and Nanostructures*, vol. 92, pp. 47–54, Aug. 2017, doi: [10.1016/j.physe.2017.05.011](https://doi.org/10.1016/j.physe.2017.05.011).
- [36] M. Tauviquirrahman et al., "Performance comparison of Newtonian and Non-Newtonian fluid on a heterogeneous Slip/No-Slip journal bearing system based on CFD-FSI method," *Fluids*, vol. 7, no. 7, p. 225, Jul. 2022, doi: [10.3390/fluids7070225](https://doi.org/10.3390/fluids7070225).
- [37] P. Thapliyal and G. D. Thakre, "Correlation Study of physicochemical, rheological, and tribological parameters of engine oils," *Advances in Tribology*, vol. 2017, pp. 1–12, Jan. 2017, doi: [10.1155/2017/1257607](https://doi.org/10.1155/2017/1257607).
- [38] M. J. Davies and K. Walters, *The behaviour of non-newtonian lubricants in Journal bearings—a theoretical study.*, T. C. Davenport. in *Rheology of Lubricants*. New York: Applied Science Publishers, 1972.
- [39] T. W. Bates, B. P. Williamson, J. A. Spearot, and C. K. Murphy, "A correlation between engine oil rheology and oil film thickness in Engine Journal bearings," *SAE Technical Paper Series*, Feb. 1986, doi: [10.4271/860376](https://doi.org/10.4271/860376).
- [40] R. Zhang and X. K. Li, "Non-Newtonian effects on lubricant thin film flows," *Journal of Engineering Mathematics*, vol. 51, no. 1, pp. 1–13, Jan. 2005, doi: [10.1007/s10665-004-1342-z](https://doi.org/10.1007/s10665-004-1342-z).
- [41] M. M. Khonsari, E. R. Booser, and F. E. Kennedy, "Applied Tribology: bearing design and lubrication," *Journal of Tribology*, vol. 124, no. 2, p. 428, Apr. 2002, doi: [10.1115/1.1432665](https://doi.org/10.1115/1.1432665).
- [42] P. J. Blau, "The significance and use of the friction coefficient," *Tribology International*, vol. 34, no. 9, pp. 585–591, Sep. 2001, doi: [10.1016/s0301-679x\(01\)00050-0](https://doi.org/10.1016/s0301-679x(01)00050-0).
- [43] S. Samion, M. Hariz, Mohd. K. Abd. Hamid, and A. R. A. Bakar, "Friction characteristic of mineral oil containing palm fatty acid distillate using four ball tribo-tester," *Procedia Engineering*, vol. 68, pp. 166–171, Jan. 2013, doi: [10.1016/j.proeng.2013.12.163](https://doi.org/10.1016/j.proeng.2013.12.163).
- [44] O. A. Aguilar-Rosas, L. I. Farfán-Cabrera, A. Erdemir, and J. A. Cao-Romero-Gallegos, "Electrified four-ball testing - A potential alternative for assessing lubricants (E-fluids) for electric vehicles," *Wear*, vol. 522, p. 204676, Jun. 2023, doi: [10.1016/j.wear.2023.204676](https://doi.org/10.1016/j.wear.2023.204676).